

Electronic Supplementary Material (ESI) for Green Chemistry.

This journal is © The Royal Society of Chemistry 2021

Electronic Supplementary Information

Highly Dispersed Ru-Co Clusters on Irrefragable N doped Carbon Shell towards Li-O₂/CO₂ Batteries and Exploiting the Synergistic Effect of O₂ and CO₂

Yuebin Lian,^{*a,b,c} Long Xiao,^{b,c} Xiaoyu Yang,^a Weilong Xu,^a Xiaojiao Du,^a Yilun Hong,^a Min Zheng,^a Yang Peng,^{*b,c}

a. School of Optoelectronic Engineering, Changzhou Institute of Technology, Changzhou 213032, P. R. China.

b. Soochow Institute for Energy and Materials Innovations, College of Physics, Optoelectronics and Energy & Collaborative Innovation Center of Suzhou Nano Science and Technology, Soochow University, Suzhou 215006, P. R. China.

c. Key Laboratory of Advanced Carbon Materials and Wearable Energy Technologies of Jiangsu Province, Soochow University, Suzhou 215006, P. R. China.

Email: lianyb@czu.cn; ypeng@suda.edu.cn

Yuebin Lian and Long Xiao contributed equally to this work.

Experimental details

Materials

Cobalt nitrate hexahydrate (Co(NO₃)₂·6H₂O, 98%) was purchased from Sinopharm Chemical Reagent Co., Ltd.. Trisodium citrate dihydrate (Na₃C₆H₅O₇·2H₂O, 99%), Potassium hexacyanocobaltate (III) (K₃Co(CN)₆, 99%) and dopamine (C₈H₁₁NO₂, 98%), were purchased from Aladdin. Ruthenium trichloride trihydrate (95%) were purchased from Sigma-Aldrich. Tris(hydroxymethylaminomethane) was purchased from Aladdin. All the received without further purification and all the solvents used were of analytical grade.

Synthesis of CoRu PBA nanocubes.

The Co-Co PBA nanocubes were synthesis by a simple precipitation method as report before.¹ solution B (0.4 mmol potassium hexacyanocobaltate (III) in 20 mL H₂O) was added to solution A (0.9 mmol trisodium citrate dihydrate, 0.6 mmol of cobalt nitrate hexahydrate in 20 mL H₂O) under magnetic stirring for 5 min. After aging for 24 h, the precipitates were collected, followed by washing with DI water and ethanol and dried at 70 °C overnight. Then, 20 mg of the pink powder was added into 20 mL solution with 2 mg RuCl₃, after string for 12 h, the dark brown suspension was collected for for subsequent use.

Synthesis of RuCo PDA-600

100 mg of the as prepared RuCo PBA nanocubes and 100 mg dopamine hydrochloride were dispersed into 20 mL of H₂O by ultrasonication for 10 min to obtain a homogeneous suspension. Then, 1 mL Tris(hydroxymethylaminomethane) solution (121 mg mL⁻¹) was added into the above solution with vigorously stirring. The obtained mixture was centrifugated and dried at 60 °C for 12 h. The as-coated RuCo PDA was annealed in Ar atmosphere at 600 °C for 2 h with a heating rate of 5 °C min⁻¹.

Acid leaching of RuCo PDA-600

20 mL 1 M HCl was added into 100 mg RuCo PDA, the mixture was then sonication for 2 h, after washed with DI water and ethanol the material was then dried at 70 °C overnight.

Characterizations

The crystalline phase of the products was analyzed by powder XRD measurements with a Bruker D8 Advance X-ray diffractometer using Cu-K α radiation and performed at a scanning rate of 0.1 s⁻¹. TGA was used to determine the optimum calcination temperature in order to obtain the best morphology and structures with EXSTAR 7300 (SII NanoTechnology). Raman spectrum analysis (Horiba HR Evolution, with laser excitation at 633 nm sweep from 200 to 2500 cm⁻¹) was used to distinguish the characteristic vibrational modes of the synthesized materials, mainly for the D-band and G-band of the carbonized samples. Brunauer-Emmett-Teller (BET, Micromeritics Tristar II 3020) analysis was used to determine the specific surface area of the catalysts. The surface elemental states of the samples were analyzed with XPS, using an Escalab 250Xi X-ray photoelectron spectrometer (Thermo Fisher) with Mg K α X-ray as the excitation source. The morphologies were examined by SEM using a Hitachi SU8010 scanning electron microanalyzer with an accelerating voltage of 10 kV. The microstructure of the samples was characterized by TEM measured at 200 kV with a FEI TECNAI G20 field-emission TEM. Elemental analysis of metal ions was determined by Inductively Coupled Plasma-Atomic Emission Spectrometry (ICP-AES) with an OPTIMA 8000 analyzer (PerkinElmer Inc.) The Fourier transformation infrared spectrum (FTIR) experiments were carried out on a Bruker Tensor 27 FT-IR spectrometer.

Battery Assembly and Testing.

The cathode was prepared by mixing 90% active material (RuCo PDA-acid) with 10% poly(vinylidene difluoride) (PVDF) in N-methyl-2-pyrrolidone dispersant. The obtained slurry was then coated onto Toray Carbon Paper (TGP-H-060) and dried at 100 °C overnight before use. A typical mass loading of the cathode catalyst was 1.5 mg cm⁻² and the specific capacity was calculated based on the total mass of the cathode catalyst. The Li-CO₂, Li-O₂/CO₂, and Li-O₂ batteries were assembled based on a coin-cell structure in an Ar-filled glovebox (H₂O < 0.1 ppm, O₂ < 0.4 ppm). The lithium foil and 0.1 M lithium perchlorate (LiClO₄) in DMSO were used as anode and electrolyte, respectively. The obtained coin cells were transferred to home-made pressure-tight glass containers and refilled with purified CO₂, O₂/CO₂ mixed gas (adjusting the ratio with flow meter), or O₂ for 20 min before test. The battery galvanostatic discharge/charge test was carried out on the LAND multichannel battery testing system at room temperature.

Table 1. The Co/Ru ratio of 2.5% RuCo PDA-acid with different

Sample	Co: Ru (EDX)	Co: Ru (ICP)	Co: Ru (XPS)
RuCo PDA-acid	4.29:1	4.50:1	4.33:1

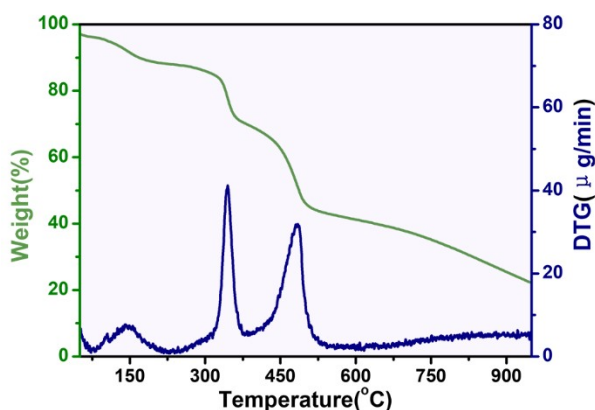


Fig. S1 a) The TGA of RuCo PDA in the nitrogen atmosphere;

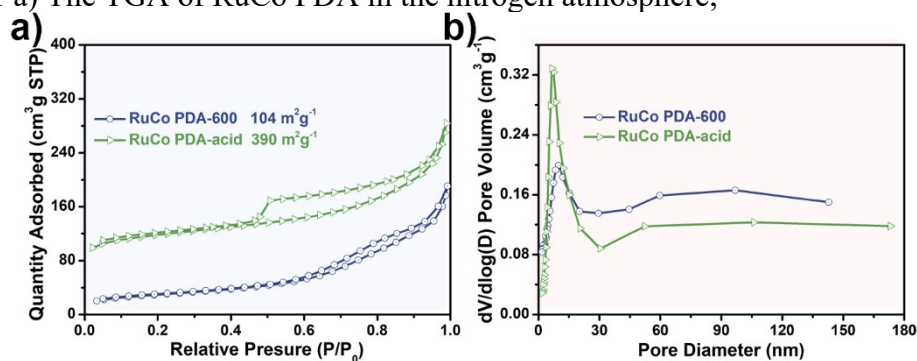


Fig.S2 a) N₂ sorption isotherms of the catalysts at 77 K; b) pore size distribution.

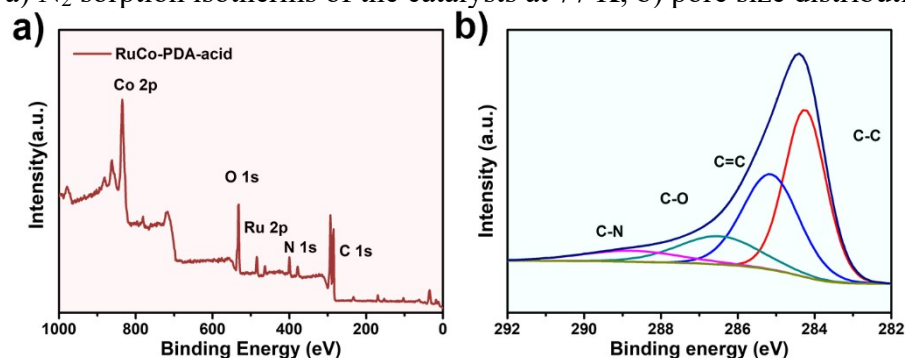


Fig. S3 a) the XPS survey spectrum of the RuCo PDA-acid; High-resolution b) C 1s XPS spectra of the RuCo PDA-acid.

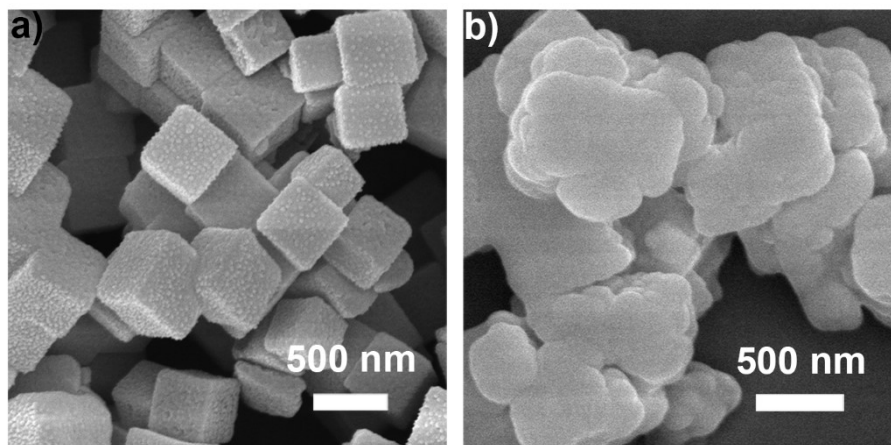


Fig. S4 The SEM image of a) normal dosage coating and b) excess dosage coating ($m_{\text{PBA}}:m_{\text{PDA}}=1:2$) of PDA.

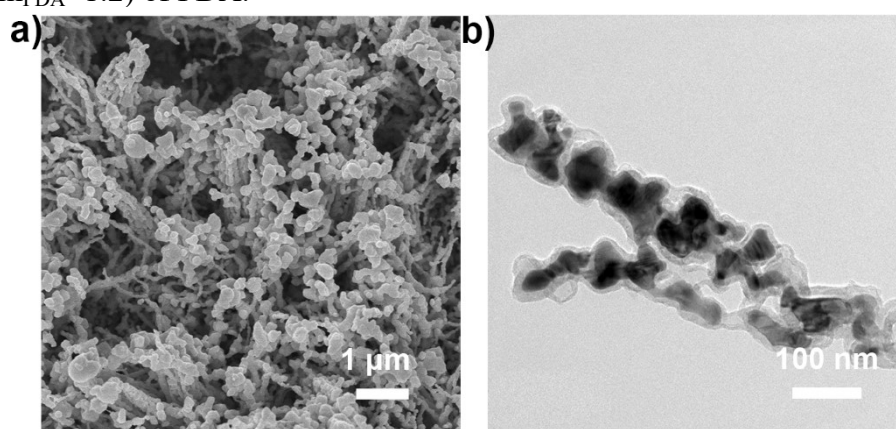


Fig. S5 The a) SEM and b) TEM image of RuCo PBA-600 without any PDA coating.

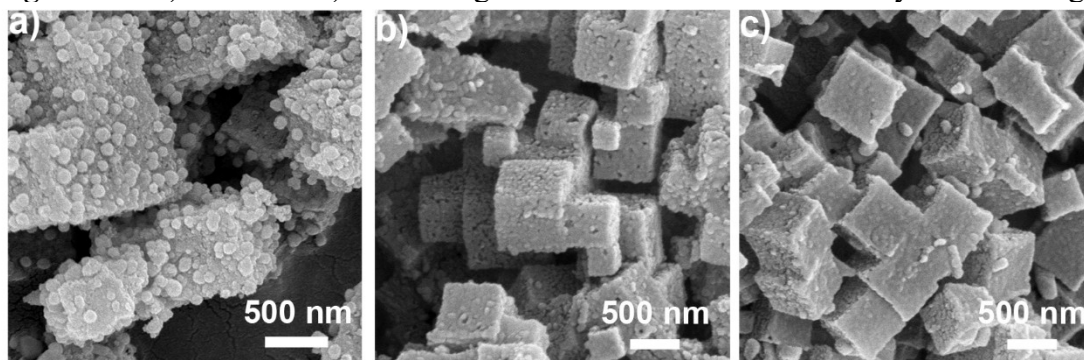


Fig. S6 The SEM image of RuCo PDA-600 with different coating dosage. a) $m_{\text{PBA}}:m_{\text{PDA}}=3:1$; b) $m_{\text{PBA}}:m_{\text{PDA}}=2:1$; c) $m_{\text{PBA}}:m_{\text{PDA}}=1:1$

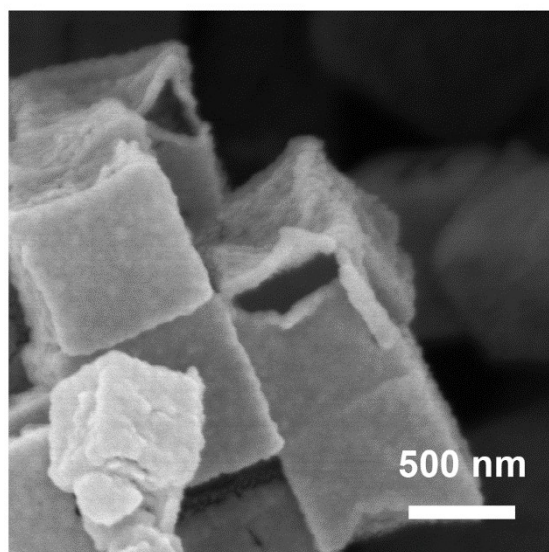


Fig. S7 a) The SEM image of RuCo PDA-acid with an opening.

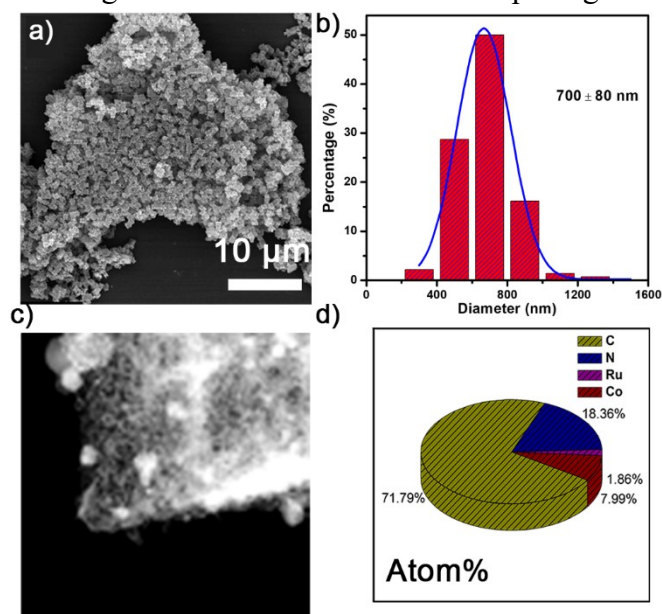


Fig. S8 a) The large area image of RuCo PDA-acid; b) Particle size distribution curve by statistics; c) High-angle annular dark-field scanning transmission electron microscope (HAADF-STEM) image of RuCo PDA-acid and d) The element content determined by EDX.

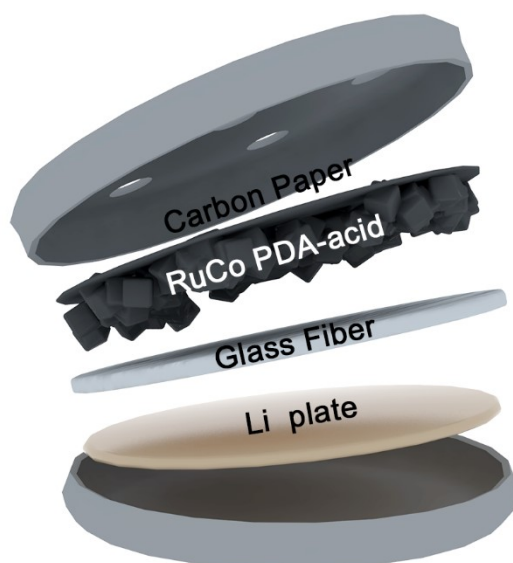


Fig. S9 The Schematic diagram structure of Li-O₂/CO₂ battery.

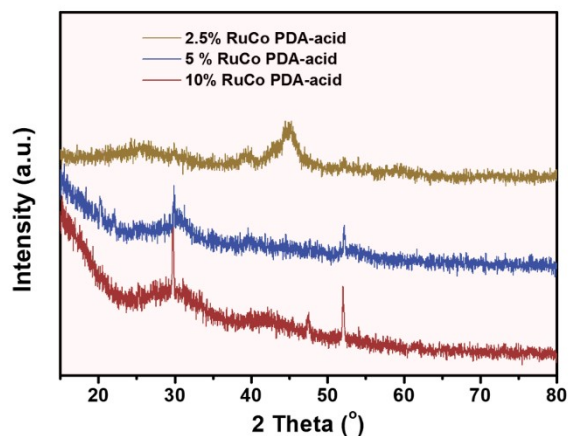


Fig. S10 The XRD of RuCo PDA-acid with different Ru dosage, the strong peaks of 10% RuCo PDA-acid and 5% RuCo PDA-acid suggests the high crystallinity and large particle size of the remaining metal alloy.

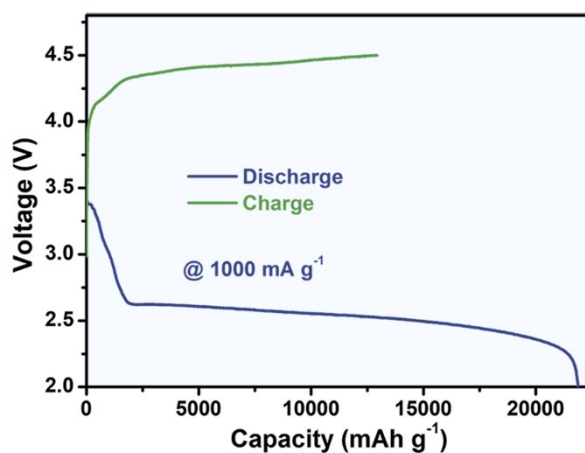


Fig. S11 The full discharge capacity of Li-O₂/CO₂ (V_{O₂}:V_{CO₂}=1:1)

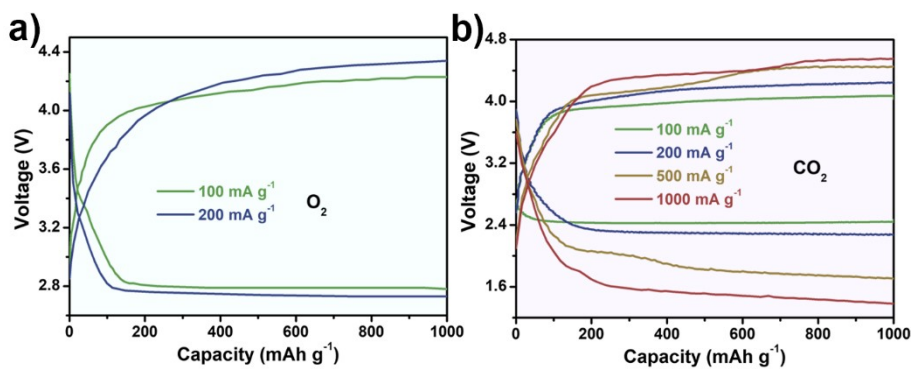


Fig. S12 The discharge/charge curves of a) Li-O₂ battery and b) Li-CO₂ battery with different current rate.

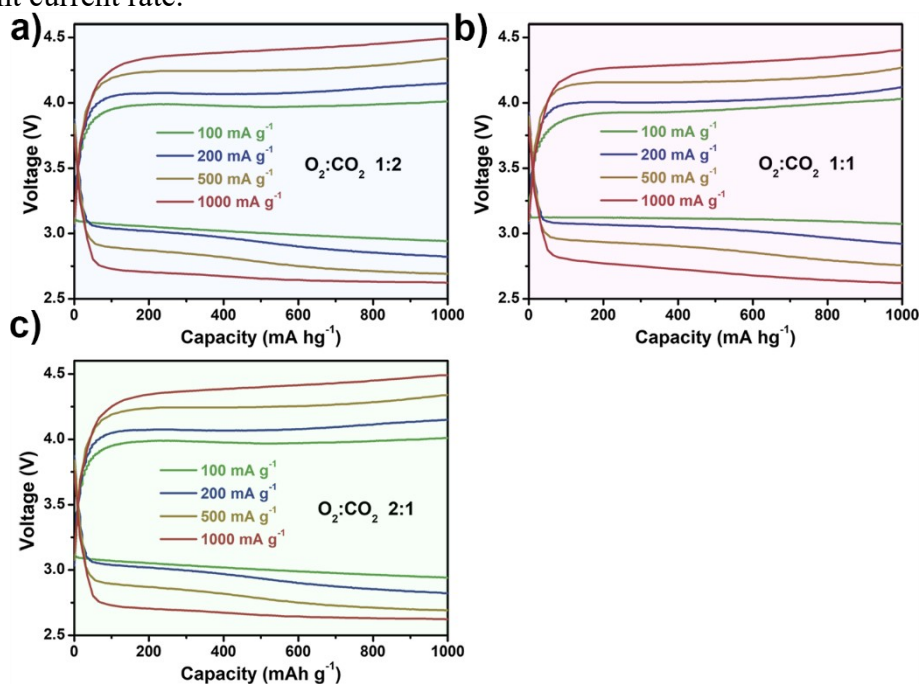


Fig. S13 The discharge/charge curves of Li-O₂/CO₂ battery Li-CO₂ battery with different ratio of O₂ to CO₂ a) $V_{O_2}/V_{CO_2}=1/2$; b) $V_{O_2}/V_{CO_2}=1/1$; c) $V_{O_2}/V_{CO_2}=2:1$.

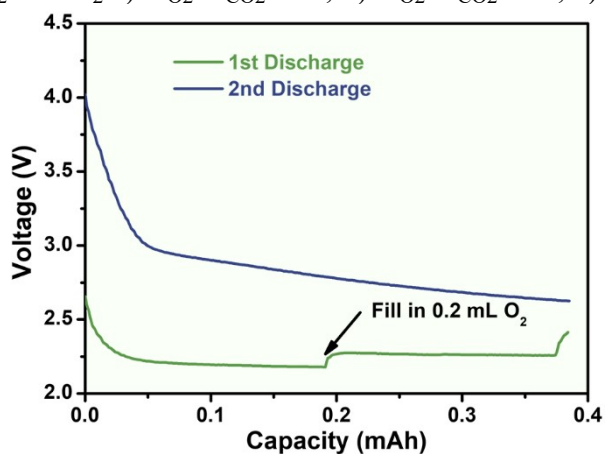


Fig. S14 The discharge curve of Li-CO₂ battery with addition of O₂ in halfway.

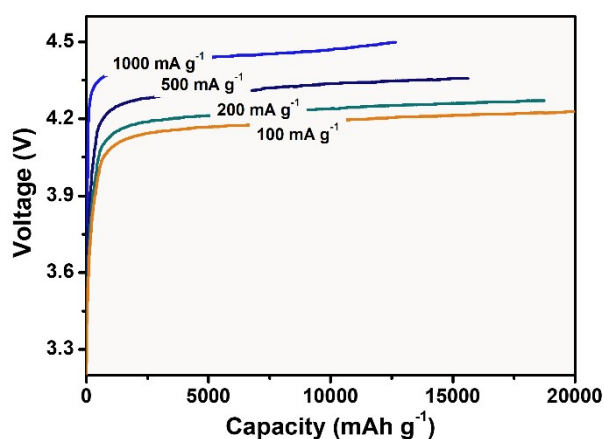


Fig. S15 The charge curve with different charge rate.

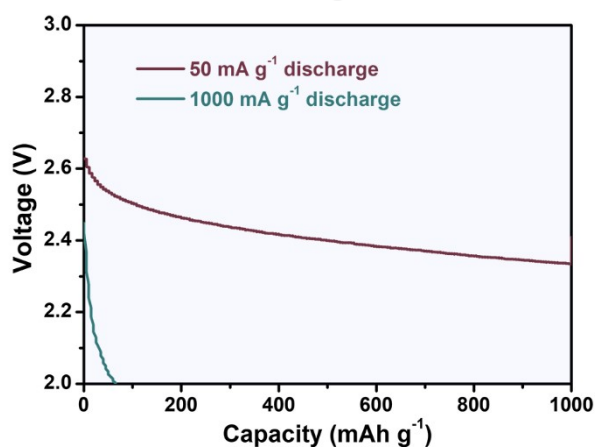


Fig.S16 The capacity of Li-Ar battery with different discharge rate.

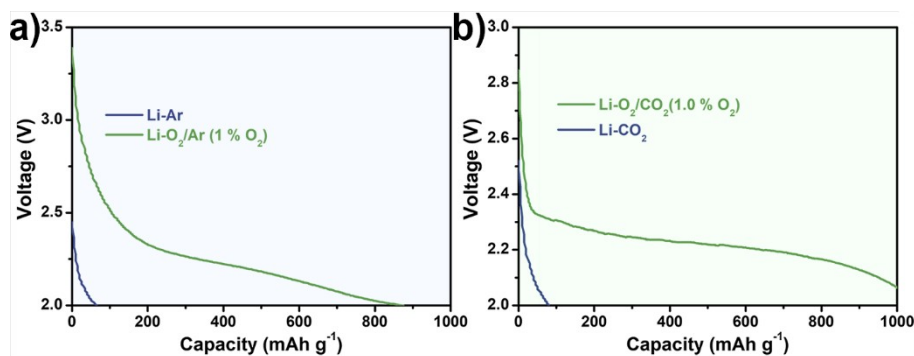


Fig. S17 The capacity of a) Li-O₂/Ar battery and b) its counterpart Li-O₂/CO₂ battery with a discharge rate of 500 mA g⁻¹, suggesting the inert nature of CO₂ during the redox process.

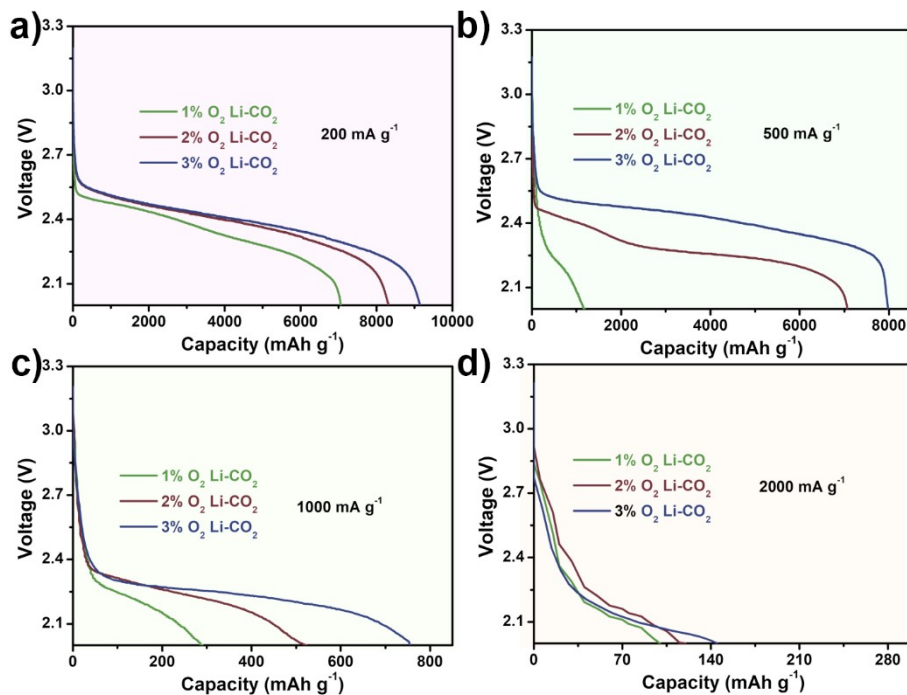


Fig. S18 The capacity of Li-O₂/CO₂ battery with 1%-3% O₂ content at a) 200 mA g⁻¹ b) 500 mA g⁻¹, c) 1000 mA g⁻¹ and 2000 mA g⁻¹ current rate.

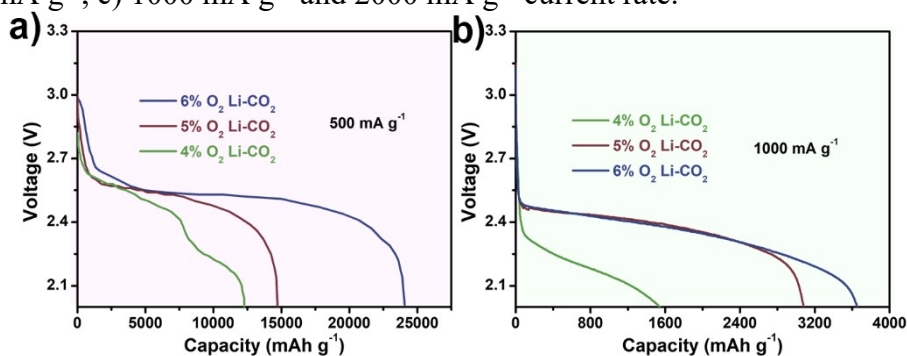


Fig. S19 The capacity of Li-O₂/CO₂ battery with 4%-6% O₂ content at a) 500 mA g⁻¹ and b) 1000 mA g⁻¹ current rate.

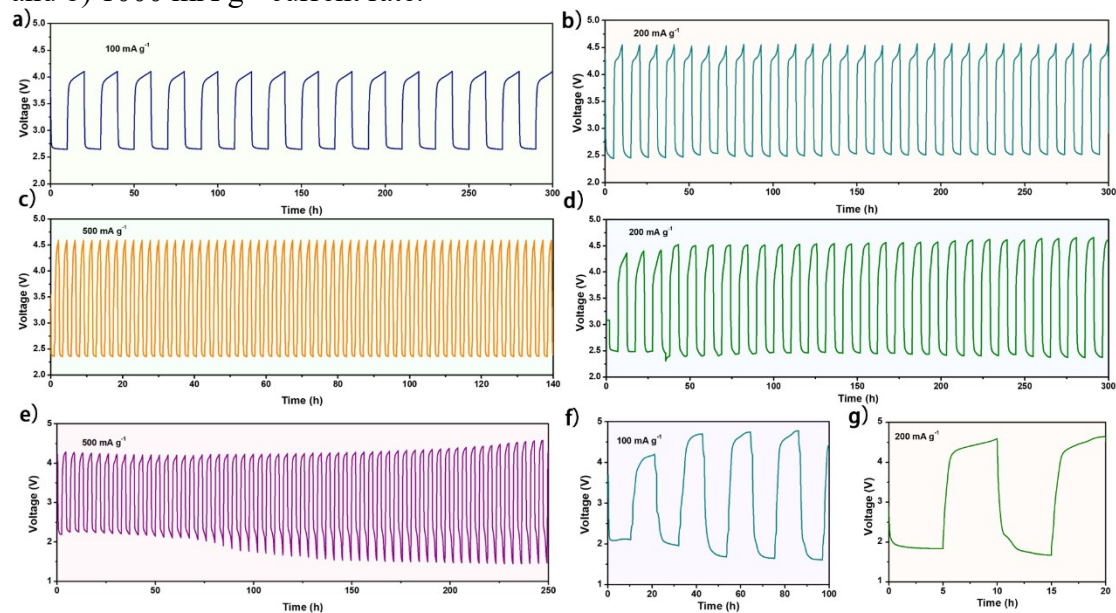


Fig. S20 The long time cyclic stability test with current rate of a) 100 mA g⁻¹, b) 200 mA g⁻¹ and c) 500 mA g⁻¹ and a limit capacity of 1000 mAh g⁻¹ in V_{O₂}:V_{CO₂}= 1:2 atmosphere; The long time cyclic stability test with current rate of d) 200 mA g⁻¹ and e) 500 mA g⁻¹ and a limit capacity of 1000 mAh g⁻¹ in CO₂ atmosphere with 5% O₂ pumping in; The cyclic stability test with current rate of f) 100 mA g⁻¹ and g) 200 mA g⁻¹ and a limit capacity of 1000 mAh g⁻¹ in CO₂ atmosphere without O₂ pumping in.